Activation-dependent clustering of the erbB2 receptor tyrosine kinase detected by scanning near-field optical microscopy

Péter Nagy[1,2,*], Attila Jenei[1,2], Achim K. Kirsch[1], János Szöllősi[2], Sándor Damjanovich[2] and Thomas M. Jovin[1,‡]

[1]Department of Molecular Biology, Max Planck Institute for Biophysical Chemistry, Am Faßberg 11, D-37077 Göttingen, Germany
[2]Department of Biophysics and Cell Biology, University Medical School of Debrecen, Nagyerdei krt. 98, PO Box 39, H-4012 Debrecen, Hungary
*Biophysical Research Group of the Hungarian Academy of Sciences, University Medical School of Debrecen
‡Author for correspondence (e-mail: tjovin@mpc186.mpibpc.gwdg.de)

SUMMARY

ErbB2 (HER2, Neu), a member of the epidermal growth factor (EGF) receptor tyrosine kinase family, is often overexpressed in breast cancer and other malignancies. ErbB2 homodimerizes but also presents as a common auxiliary subunit of the EGF and heregulin receptors (erbB1 or EGFR; and erbB3-4, respectively), with which it heteroassociates. ErbB2 is generally regarded as an orphan (ligand-less) receptor with a very potent kinase domain activated either via its associated partners or constitutively as a consequence of discrete mutations. It follows that the extent and regulation of its cell surface interactions are of central importance. We have studied the large-scale association pattern of erbB2 in quiescent and activated cells labeled with fluorescent anti-erbB2 monoclonal antibodies using scanning near-field optical microscopy (SNOM). ErbB2 was found to be concentrated in irregular membrane patches with a mean diameter of approx. 0.5 μm in nonactivated SKBR3 and MDA453 human breast tumor cells. The average number of erbB2 proteins in a single cluster on nonactivated SKBR3 cells was about 10^3. Activation of SKBR3 cells with EGF, heregulin as well as a partially agonistic anti-erbB2 monoclonal antibody led to an increase in the mean cluster diameter to 0.6-0.9 μm, irrespective of the ligand. The EGF-induced increase in the erbB2 cluster size was inhibited by the EGFR-specific tyrosine kinase inhibitor PD153035. The average size of erbB2 clusters on the erbB2-transfected line of CHO cells (CB2) was similar to that of activated SKBR3 cells, a finding correlated with the increased base-line tyrosine phosphorylation of erbB2 in cells expressing only erbB2. We conclude that an increase in cluster size may constitute a general phenomenon in the activation of erbB2.

Key words: ErbB2; EGF receptor; Homassociation; SNOM; NSOM

INTRODUCTION

ErbB2 is a member of the epidermal growth factor receptor (EGFR) family of transmembrane receptor tyrosine kinases (Alroy and Yarden, 1997; Hynes and Stern, 1994). Although it has no known ligand, it is commonly found in heteroassociation with the other three members of the erbB family, specifically the EGF (erbB1) and heregulin (erbB3, erbB4) receptors (Karunagaran et al., 1996). The interaction with erbB2 greatly enhances the signaling capacity of these proteins (Tzahar et al., 1996). Mutant forms of erbB2 are highly oncogenic due to the constitutive activation of its very potent kinase activity (Bargmann et al., 1986). The effects of oncogenic erbB2 on the malignant phenotype are also determined by the nature of the homo- and heterodimers that form in the context of a given expression pattern. ErbB2 is overexpressed in breast cancer patients (Ahmad et al., 1993). However, considerable controversy exists about the prognostic value of this finding, attributable at least in part to differences in the binding specificities and affinities of the monoclonal and polyclonal antibodies used in clinical laboratory practice (Press et al., 1994; Strawn and Shawver, 1998). The importance of small- and large-scale clustering of receptors in determining the malignant phenotype was not addressed in these studies. A humanized monoclonal antibody against erbB2 has been in clinical trial (Baselga et al., 1996) and just approved for patient use.

The association of erbB receptor molecules has been examined extensively by classical biochemical, molecular biological (Sliwkowski et al., 1994; Tzahar et al., 1996) and biophysical (Gadella and Jovin, 1995; Nagy et al., 1998) techniques. Biochemical methods revealed that extensive homo- and heteroassociation is present among members of the erbB family (Tzahar et al., 1996), but since these methods necessitate the isolation of proteins, they are inherently unable to detect the association in the in vivo environment, and are also not suitable for detecting heterogeneity within or among cells. Fluorescence resonance energy transfer (FRET) has been used to measure the monomer-dimer distribution of EGF (erbB1) receptors in living cells (Gadella and Jovin, 1995), as

well as the heterogeneous pattern of erbB2 association in breast tumor cells (Nagy et al., 1998). The homoassociation of erbB2 was heterogeneous in unstimulated SKBR3 breast tumor cells; membrane areas with a mean diameter in the sub-μm range were present, in which the extent of homoassociation was anomalously high (Nagy et al., 1998). The implication is that large-scale association of receptors may exist, in addition to dimerization. Unfortunately, the resolution power of the conventional fluorescence microscope has not permitted a more detailed analysis of this phenomenon. In short, the methods employed to date have been restricted to the very high and to the very low limits of the detection scale, corresponding to physical interactions at the level of homo- and heterodimers or extensive molecular associations (caps and patches), respectively.

Numerous studies directed at the plasma membrane have provided evidence for the existence of distinct domains in the sub-μm range (Damjanovich et al., 1995; Edidin, 1997; Friedrichson and Kurzchalia, 1998; Hwang et al., 1998, 1995; Jacobson et al., 1995; Jenei et al., 1997; Kenworthy and Edidin, 1998; Varma and Major, 1998; Vereb et al., 1997). These patches are found for lipids ('rafts') as well as protein molecules, the distribution patterns of which do not necessarily overlap (Hwang et al., 1998). In the case of the major histocompatibility complex class I (MHC-I), clusters containing 50-100 molecules have been reported (Hwang et al., 1998; Matkó et al., 1994).

Protein-protein interactions among erbB proteins are important. However, the formation of large associations with dimensions in the range of several hundred nm has been neglected so far in the study of the erbB signaling network. Since a local accumulation of a growth factor receptor may enhance the efficiency of transmembrane signaling, e.g. by providing a 'focusing effect', we examined the distribution of erbB2 protein in the plasma membrane of cells and established a correlation between the degree of clustering with the activation state of the protein.

The FRET phenomenon is inherently very sensitive to dimerization (Gadella and Jovin, 1995) and global surface distribution patterns (Kenworthy and Edidin, 1998; Varma and Major, 1998), but not to the evolution of higher order complexes during a process such as clustering. In contrast to FRET, the newly available technique of scanning near-field optical microscopy (SNOM) is not limited by diffraction optics, and one can readily image objects in the 0.1-1 μm range, including sub-μm lipid and protein clusters in the plasma membrane (Hwang et al., 1998, 1995; Kirsch et al., 1996; Nagy et al., 1998; Vereb et al., 1997). In this study, we used fluorescent anti-erbB2 antibody-labeled samples and SNOM to detect and characterize the clustering of erbB2 on the surface of quiescent and activated cells. ErbB2 formed very conspicuous patches in the plasma membrane of two different breast tumor cells (SKBR3 and MDA453), the mean diameter of which was approx. 0.5 μm. Cluster formation may be a general property of erbB2, since it was also present in the plasma membrane of erbB2-transfected CHO cells. However, the size of the erbB2 clusters was considerably larger in these cells. We attribute this finding to the higher baseline tyrosine phosphorylation (activation) level of erbB2 in cells expressing only erbB2, inasmuch as activation of SKBR3 breast tumor cells with EGF, heregulin and a partially agonistic antibody

(4D5) also resulted in an increase in cluster size. The causal relationship between activation of erbB signaling and increased cluster size was further corroborated by the finding that the EGF-induced effect on the mean size of erbB2 clusters was blocked by the EGF receptor-specific quinazoline-based PD153035 tyrosine kinase inhibitor.

MATERIALS AND METHODS

Cell lines

Human breast tumor cell lines SKBR3 and MDA453 were obtained from the American Type Tissue Culture Collection (Rockville, MD) and grown according to specified protocols to confluency on the surface of glass coverslips. CB2 cells generated by transfecting erbB2 into Chinese Hamster Ovary (CHO) cells (Tzahar et al., 1996), were kindly provided by Y. Yarden (Weizmann Institute, Rehovot, Israel).

Antibodies and calibration microspheres

Two antibodies directed against non-overlapping extracellular epitopes on erbB2 (4D5, 7C2) were a generous gift of Genentech (Genentech Inc., South San Francisco, CA) (Fendly et al., 1990). Monovalent Fab fragments were generated from the 4D5 antibody as described previously (Nagy et al., 1998). Samples of purified monoclonal antibodies or Fab fragments were labeled with 5-(and 6-)carboxytetramethylrhodamine succinimidyl ester (TAMRA-SE, Molecular Probes, Eugene, OR) according to standard protocols provided by the manufacturer. The dye:protein ratio was 3:1 and 1:1 in the case of antibodies and Fab fragments, respectively, and was determined by spectrophotometric methods. Fluorescently-tagged antibodies and Fab fragments retained their binding capacity, according to competition assays with identical, but unlabeled antibodies.

The integrated fluorescence intensity of single erbB2 clusters was quantitated by comparison with Rainbow Calibration Particles (Spherotech Inc., Libertyville, IL).

Labeling of cell-surface antigens

Cells were used for labeling and SNOM and confocal microscopic imaging on the surface of glass coverslips without trypsinization (in situ labeling). They were washed twice in phosphate-buffered saline (PBS), and labeled with a saturating concentration of a monoclonal antibody or Fab fragment for 30 minutes on ice in the dark. Excess, unbound monoclonal antibody or Fab fragment was removed by washing the cells twice in ice-cold PBS. Cells for SNOM imaging were then fixed in 4% paraformaldehyde for 60 minutes on ice, and dehydrated in an ethanol series. Experiments with a confocal microscope were carried out with non-dehydrated cells that were either unfixed or mildly fixed in 1% paraformaldehyde for 30 minutes on ice.

Activation of cells with EGF, heregulin and 4D5 antibody

Cells were treated with 50 ng/ml EGF or 50 ng/ml heregulin (the EGF-like domain of heregulin alpha, R&D Systems, Abingdon, UK) in situ on the surface of coverslips. Cells were kept in a CO_2 incubator at 37°C for 30 minutes in medium without serum in the presence of the activating agents. Cells were then washed twice in PBS, and labeled with fluorescent antibodies as described above.

Activation with the 4D5 antibody was carried out as follows. Cells were incubated in the presence of a saturating concentration of TAMRA-labeled 4D5 antibody for 30 minutes at 37°C in a CO_2 incubator in medium without serum. Then cells were washed twice in PBS, fixed and dehydrated as described above, and imaged with the SNOM. In this case, the activating and the labeling antibodies were the same. In another protocol we used a saturating concentration of unlabeled 4D5 antibody as the activating agent. After incubating the cells in the presence of unlabeled 4D5 for 30 minutes at 37°C in the CO_2 incubator in medium without serum, cells were washed twice in

PBS, and labeled with TAMRA-labeled 7C2 anti-erbB2 antibodies as described above. Afterwards these cells were also fixed and dehydrated before imaging. Since 4D5 treatment induces internalization of erbB2 (Sarup et al., 1991), this second protocol ensured that the fluorescent labels were restricted to the extracellular surface of cells, i.e. were not binding to endocytotic vesicles.

Treatment of cells with kinase inhibitor

The quinazoline-based PD153035 tyrosine kinase inhibitor (4-[(3-bromophenyl)amino]-6,7-dimethoxyquinazoline) was purchased from Calbiochem (Bad Soden, Germany). Because of the low aqueous solubility, a stock solution (2 mM) was prepared in THF and diluted before treatment. Cells were exposed in the presence of PD153035 in 1 µM final concentration for 5 minutes at 37°C in a CO_2 incubator in medium without serum. The EGF activation was carried out in the presence of the inhibitor specified above.

Scanning near-field optical microscopy (SNOM)

The SNOM was an add-on to a Nanoscope-IIIa scanning probe system (Digital Instruments, Santa Barbara, CA) (Kirsch et al., 1998a). Simultaneous excitation and detection of fluorescence emission were with an uncoated optical fiber tip (Bielefeldt et al., 1994; Courjon et al., 1990; Kirsch et al., 1998a,b). The tips were produced with a commercial pipette puller (P-2000, Sutter Instruments, Novato, CA) from a 9 µm core diameter optical fiber (SMF 1528 CPC6, Siecor, Neustadt, Germany) and mounted in a shear force sensor head developed in our laboratory (Kirsch et al., 1997). Excitation of the TAMRA-labeled monoclonal antibodies was with the 543 nm line of an He-Ne laser (LHGP 0101, Research Electro Optics, Boulder, CO). Fluorescence was detected through a 488/543 nm dichroic mirror (Chroma Techn., Brattleboro, VT) and a SWP 605/55 nm bandpass filter (Chroma Techn.). In addition, a 630/30 nm bandpass filter (Omega Optical Co., Brattleboro, VT) was included to block stray light from the red diode laser used for shear force detection.

Image analysis

Cluster size analysis was performed by three different techniques.

Method 1

The cluster diameter of clusters (also referred to as particles below) was determined manually after judiciously positioning the cursor on the screen on opposing edges of the fluorescent region. Frequency histograms were constructed from at least 200 such data points.

Method 2

The original image was low-pass filtered and divided into the original image, thereby obtaining an image lacking most background intensity variations (Hwang et al., 1998). The resultant image was segmented using the entropy threshold algorithm of Scil-Image (Technical University of Amsterdam, The Netherlands). The distribution of particle sizes on this binary mask image was determined by ScionImage (Scion Corp., Frederick, MA). A frequency histogram was generated from cluster areas comprising at least 200 particles.

Method 3

Normalized two-dimensional spatial autocorrelation functions (Hwang et al., 1998) were computed by taking the inverse Fourier-transform of the two-dimensional power spectrum matrix of the original image. The rotation-invariant autocorrelation function was obtained by averaging overall angles of the spatial lag vector, and fitted to the formula:

$$g(\xi) = \sum_i gi(\xi) \exp[-(\xi/\xi_i)^2]$$

where $g(\xi)$ is the angle-averaged autocorrelation function, ξ is the spatial lag vector, i and ξ_i is the characteristic radius, which serves as an adequate measure of the mean size of a single class of clusters

(Hwang et al., 1998). Fitting was carried out with Microcal Origin v.5 (Microcal Software Inc., Northampton, MA). The best fits were obtained using two different characteristic radii. One of the terms was taken as a measure of the average cluster size, since its value was in the range of the directly observed clusters. We attributed the second term with values of 2-5 µm to a low frequency trend in the background fluorescence intensity or to clustering of clusters; it was consequently not considered further in the interpretation of results.

The fluorescence color-coded surface plots were generated with SXMImage (Swiss Center for Electronics and Microtechnology, Inc., Neuchatel, Switzerland).

Confocal microscopy

A Zeiss LSM410 confocal laser scanning microscope system was uesd to image non-dehydrated SKBR3 cells. Excitation of TAMRA-labeled monoclonal antibodies was carried out with the 543 nm line of a HeNe laser. Detection of fluorescence was through a 560 nm dichroic mirror and a 570 nm long-pass filter.

RESULTS AND DISCUSSION

SNOM reveals erbB2 clusters in quiescent SKBR3 cells

We have previously characterized the clustering of erbB2 on SKBR3 breast tumor cells using flow and image cytometric energy transfer measurements (Nagy et al., 1998). The SKBR3 cell line overexpresses erbB2 (~10^6 molecules/cell), but EGFR and erbB3 are present at non-amplified levels (~10^5) (Beerli et al., 1995). In the current work the same fluorescent monoclonal antibodies and a SNOM were used to characterize the distribution of erbB2 on the surface of resting and activated cells.

Quiescent SKBR3 cells were labeled with TAMRA-tagged anti-erbB2 antibodies and imaged with the SNOM (Fig. 1). The distribution of erbB2 was conspicuously uneven (Fig. 1B); the fluorescence of the TAMRA-labeled monoclonal antibodies was concentrated in membrane patches with a diameter of ~0.5 µm (Table 1). The shear-force topography (Fig. 1A) and the fluorescence (Fig. 1B) images were merged into a composite three-dimensional representation in which height represents vertical displacement (topography) and superposed color (black increasing to bright) the fluorescence intensity (Fig. 1C). A significant tendency for the fluorescence to be greater at the 'peaks' and 'ridges' is apparent, implying that clustered receptors located in such regions would be most exposed to the extracellular milieu. We note that the SNOM technique is unique in its ability to render minute topographical features in combination with probe-specific fluorescence. A higher resolution image (rendered as top view) of quiescent SKBR3 cells is shown in Fig. 2A. The calculation of the mean fluorescence intensity of a cluster-free plasma membrane indicated that approx. 60% of the total fluorescence originated from clusters. The background intensity of unstained control cells was negligible compared to fluorescent antibody-labeled cells (data not shown).

As a next step we determined the size distribution of erbB2 clusters on the surface of quiescent SKBR3 cells. Following method 1 (Materials and methods), the diameter of single clusters was measured manually and a frequency distribution generated (Fig. 3). The erbB2 clusters on SKBR3 cells had a mean diameter of 0.48±0.08 µm, a value close to that reported earlier for another transmembrane receptor protein, MHC-I
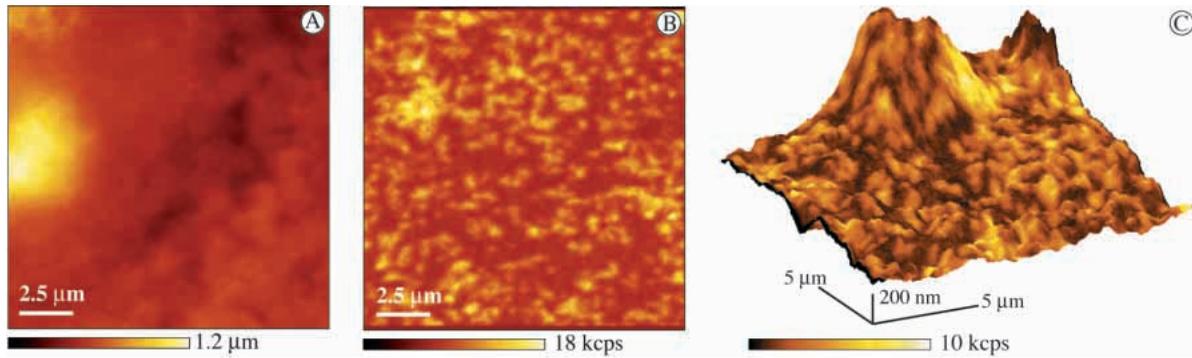
Fig. 1. SNOM images of quiescent SKBR3 cells stained with TAMRA-tagged anti-erbB2 (4D5). (A) Shear force topography. (B) Immunofluorescence. (C) Composite topography (height) and fluorescence (color coded) data. See text for details.

(Hwang et al., 1998). We segmented the images (method 2) and determined the frequency distribution of 'particle' sizes (Fig. 4). The results provided by this approach (mean cluster area: 0.27 ± 0.12 μm^2, corresponding to the diameter of an equivalent circle of 0.59 ± 0.16 μm) were in good agreement with those obtained by method 1. In method 3 we calculated the spatial autocorrelation image of TAMRA-4D5-stained SKBR3 cells (Fig. 5). One component of the fit to the angle-averaged autocorrelation function (characteristic radius of 0.36 ± 0.08 μm) was close to the cluster diameter obtained by the previous two methods. The other component, which was also present in background-corrected images, was 2-5 μm and probably reflected low frequency trends in the fluorescence image. The value of this characteristic radius did not depend on cell type or activating condition and was therefore neglected in the interpretation of the results.

Labeling of cell surface antigens might generate crosslinking even if labeling is carried out on ice in the

Table 1. Determination of erbB2 cluster diameter on quiescent and activated cells

Cells and treatments	Manual (μm)	Segmentation (μm)	Autocorrelation (μm)
SKBR3			
Quiescent	0.48 ± 0.08	0.59 ± 0.16	0.36 ± 0.08
Quiescent, labeled with Fab	0.45 ± 0.08	0.62 ± 0.07	0.42 ± 0.12
4D5-activated	$0.62 \pm 0.11*$	$0.75 \pm 0.26*$	$0.63 \pm 0.21*$
EGF-activated	$0.60 \pm 0.11*$	$0.8 \pm 0.31*$	$0.60 \pm 0.12*$
EGF-treated, in the presence of PD153035	0.39 ± 0.09	0.49 ± 0.12	0.29 ± 0.06
Heregulin-activated	$0.66 \pm 0.14*$	$0.86 \pm 0.31*$	$0.84 \pm 0.20*$
MDA453			
Quiescent	0.51 ± 0.09	0.61 ± 0.18	0.40 ± 0.08
CB2			
Quiescent	$0.83 \pm 0.13*$	$0.95 \pm 0.31*$	$0.71 \pm 0.18*$

Cells were stained with TAMRA-labeled anti-erbB2 monoclonal antibodies or with Fab if indicated, and activated with the indicated agents as described in Materials and methods.

Manual (method 1): determination of cluster size by measuring the diameter of particles on the screen.

Segmentation (method 2): entropy thresholding of background-filtered images.

Autocorrelation (method 3): determination of the angle-averaged autocorrelation function of the images.

Indicated values are means ± s.d. of at least three different experiments.

Asterisks indicate significant difference ($P<0.05$) from untreated SKBR3 cells using Student's t-test.

presence of excess antibody to ensure at least partly monomeric binding. To exclude this possibility we labeled quiescent SKBR3 cells with TAMRA-tagged 4D5 Fab fragments (Fig. 2B, Table 1). The observed diameter of erbB2 clusters did not differ from that observed with whole antibodies. In addition, we also tested whether crosslinking of 4D5 antibodies with TAMRA-labeled secondary antibodies had any effect on the cluster size. None was observed, presumably because labeling was carried out on ice (data not shown). We conclude that cluster diameter is not altered by the use of whole antibodies.

It has been reported that about 25-125 MHC-I are found in a single cluster (Hwang et al., 1998). This finding prompted us to determine the number of clustered erbB2 molecules in nonactivated SKBR3 cells. The first approach directed at the imaging of single antibody molecules did not succeed, possibly due to the lower collecting efficiency of our shared aperture SNOM system compared to instruments incorporating high numerical aperture objectives. Based on the assumption that if the antibodies could not be visualized, i.e. that their signal was in the range of the standard deviation, we estimated that about 2000 erbB2 proteins could be present in a cluster. As a second approach we used standard fluorescent microspheres to calibrate the fluorescence intensity of a single erbB2 cluster. The mean diameter of the beads was 2.5 μm, implying that their total volume was not imaged by the SNOM, for which the $1/e$ decay length in fluorescence detection is ~0.6 μm (Kirsch et al., 1998c). Since the fluorochromes were distributed evenly in the beads, we estimated that ~20% of the total nominal integrated fluorescence intensity of a given bead was detected. The bead sample consisted of microspheres with six graded, calibrated fluorescence levels, expressed in R-phycoerythrin (R-PE) equivalent units.

We measured the emission spectra of TAMRA and the bead and the excitation spectra of R-PE and TAMRA. Correcting for the transmission and reflectance profiles of the filters and dichroic mirrors, respectively, as well as the labeling stoichiometries of the antibodies, we established a calibration curve for the determination of the number of TAMRA molecules in a single cluster. On this basis we concluded that about 10^3 erbB2 proteins are present in a single cluster. A third, independent estimation of the number of erbB2 protein molecules/cluster was made from the determination that the number of erbB2 clusters is 300-400 on unactivated SKBR3 cells, assuming a homogeneous surface distribution. Confocal
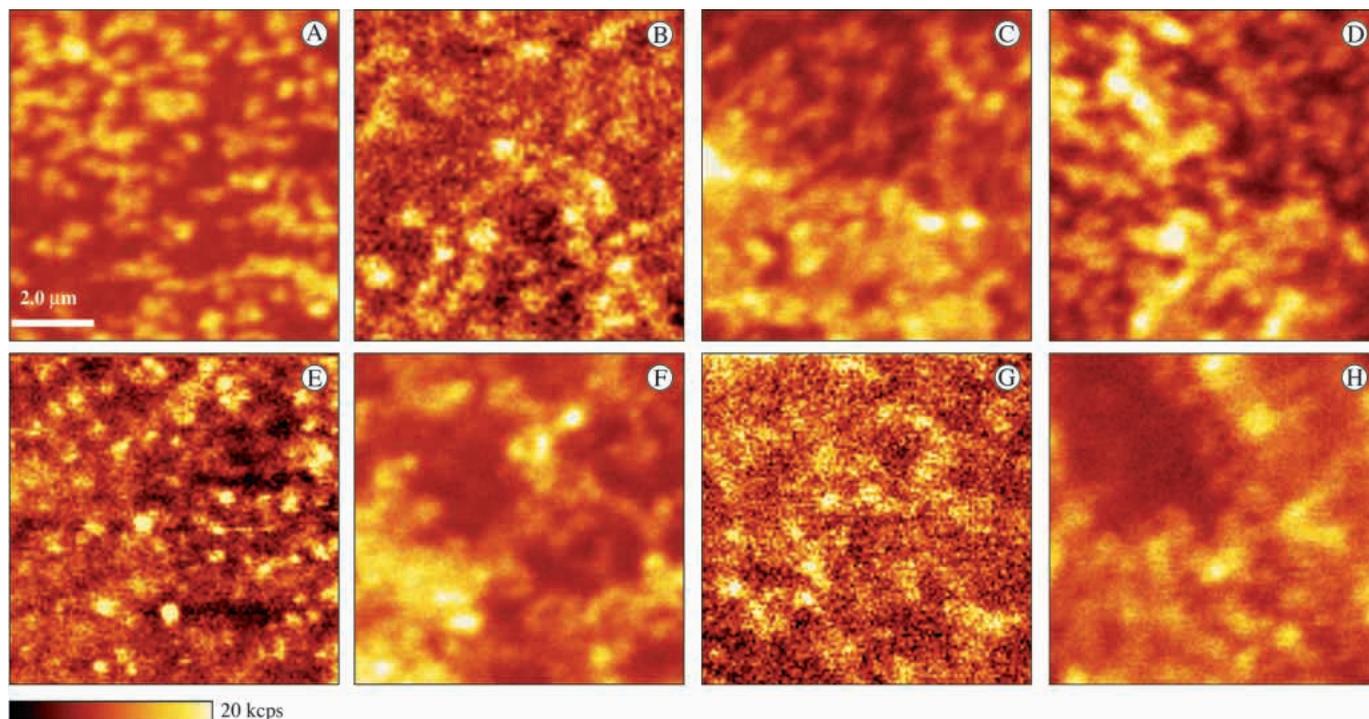
Fig. 2. SNOM images of TAMRA-tagged anti-erbB2 labeled quiescent and activated cells. (A) Quiescent SKBR3 cells stained with TAMRA-4D5 antibody. (B) Quiescent SKBR3 cells stained with TAMRA-4D5 Fab. (C) Unlabeled 4D5-activated SKBR3 cells labeled with TAMRA-tagged 7C2 antibody. (D) EGF-activated SKBR3 cells stained with TAMRA-4D5 antibody. (E) SKBR3 cells stimulated with EGF in the presence of PD153035. (F) Heregulin-activated SKBR3 cells stained with TAMRA-4D5 antibody. (G) Quiescent MDA453 cells stained with TAMRA-4D5 antibody. (H) Quiescent CB2 cells stained with TAMRA-4D5 antibody.

microscopy did not reveal significant differences in the density of erbB2 clusters in the exposed and surface-attached plasma membranes (data not shown). Since the number of erbB2 on a single SKBR3 cell is about 10^6 (Sarup et al., 1991), there should be around 1500-2000 erbB2 per cluster, based on our determination that ~60% of the fluorescence signal originates from the clusters.

We conclude that in addition to small-scale association of erbB2 on quiescent SKBR3 cells (e.g. the presence of direct protein-protein contacts revealed by resonance energy transfer), there is evidence for the large-scale clustering of this protein. Since the number of erbB2 proteins in a single cluster is quite large, it is plausible that proteins are not held together solely by direct erbB2-erbB2 interactions, but that lipid domains and extra-membrane constraints are also involved. It is also unknown how small erbB2 associations (e.g. dimers, trimers) are organized within a cluster. Inasmuch as the diameter of the clusters was not influenced by the labeling conditions (primary antibody or Fab, or secondary antibody), we infer that the clusters were not generated by extraneous antibody generated crosslinking. Future near-field energy transfer measurements of the homoassociation of erbB2 should clarify this point.

ErbB2 clustering in other cell lines

Since cell-surface distribution of a membrane protein may be cell-type dependent, we tested whether the large-scale clustering of erbB2 is also present in the context of other membrane proteins or if it is peculiar to SKBR3 cells. We chose another breast tumor cell line (MDA453), which expresses the complete erbB family (erbB1-4) except erbB1 at a level of about 10^5 copies/cell. MDA453 breast tumor cells were stained with the TAMRA-4D5 antibody according to the same protocol employed with SKBR3 cells (Fig. 2G). Although the signal intensities of the patches were much lower in these compared to SKBR3 cells (reflected in the higher relative background in image Fig. 2G), the dimension of the clusters on MDA453 was comparable to that of SKBR3 cells according to all three methods of analysis (Table 1; Figs 3, 4). Since the number of erbB2 proteins in single SKBR3 and MDA453 cells is different, as is the number of erbB2 molecules in clusters on SKBR3 and MDA453 cells, we conclude that the cluster size was independent both of the total number of erbB2 proteins expressed per cell and the number of erbB2 molecules in a single cluster.

As a next step we chose an erbB2-transfected CHO cell line (CB2) to establish whether clustering is an inherent property of erbB2. CHO cells lack endogenous expression of erbB1, erbB3 and erbB4, and express only a small number of erbB2 molecules (Tzahar et al., 1996). Thus, the only member of the erbB family in CB2 cells is erbB2. In comparison to the other cell lines, the size of the erbB2 clusters in CB2 was significantly larger (Table 1; Figs 2H, 3, 4), although the expression level of erbB2 in CB2 is lower than in MDA453 cells. According to method 1 (Fig. 3) the cluster population distribution on CB2 cells was shifted to higher values, whereas the analysis by method 2 (Fig. 4) yielded a more pronounced overlap between the frequency histograms of SKBR3 and CB2 cells. This discrepancy is probably attributable to the different sensitivities of the two methods with respect to edge detection.
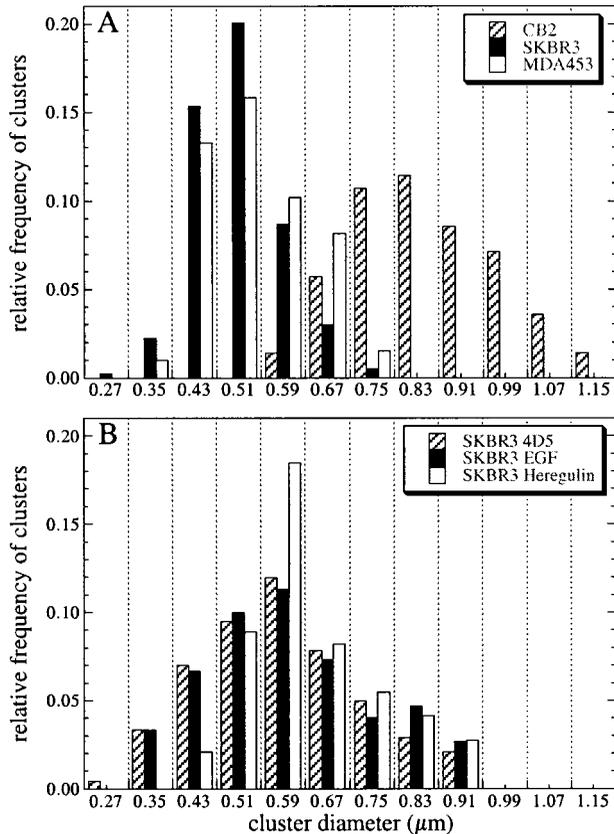
Fig. 3. Distribution of erbB2 cluster diameter in quiescent and stimulated cells. Quiescent (A) and heregulin-activated (B) cells were stained with TAMRA-labeled 4D5 antibodies, and the diameter of clusters was determined by measuring the distance between opposite edges of a particle (method 1). Frequency distributions were made from at least 200 clusters from 3 independent experiments.

Fig. 4. Distribution of erbB2 cluster area in quiescent and activated cells. Quiescent (A) and heregulin-activated (B) cells were treated with TAMRA-labeled 4D5 antibodies, and the area of clusters was determined by automatic segmentation of background-corrected images (method 2). Frequency distributions of at least 200 clusters from 3 independent measurements are presented. The histograms of heregulin- and EGF-activated cells were similar to that of 4D5-activated cells and are therefore omitted for clarity.

It has been reported that when erbB2 is expressed on its own, the constitutive basal tyrosine phosphorylation level of the protein increases compared to the situation prevailing when the other members of the erbB family are co-expressed (Tzahar et al., 1996; Wallasch et al., 1995). This phenomenon is possibly caused by the competition of other erbB proteins associating with erbB2. Since erbB2 has the highest baseline tyrosine kinase activity, the heteroassociation of erbB2 with other proteins at the expense of erbB2 homoassociation should reduce the activation of this protein. Thus, we tentatively propose that the constitutively larger cluster size in CB2 cells reflects the higher baseline activation state of erbB2 in these cells, compared to SKBR3 and MDA453. Furthermore, as the number of erbB2 molecules in an average cluster on CB2 cells was only about 2% of that in SKBR3 clusters, we infer that it is the dimension of a cluster, and not the number of erbB2 protein it encompasses, that correlates with the activation state of erbB2. The further implication is that other associated proteins (receptors, protein kinase substrates, downstream effectors) are also involved. Since the clustering of erbB2 was present on cell lines with completely different complements of membrane proteins, we presume that the patchy distribution of erbB2 is an inherent property of the receptor.
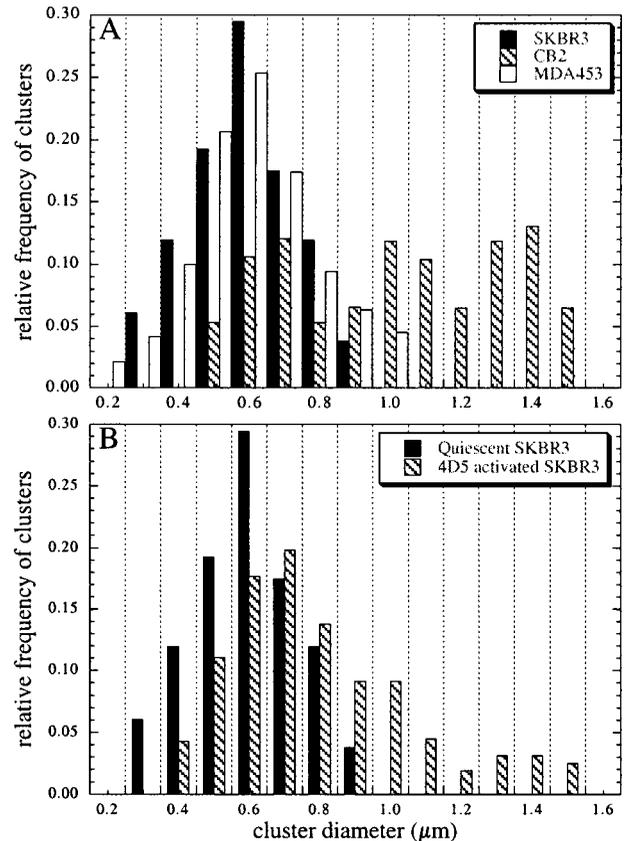
ErbB2 clustering as a function of activation and activation agent

To further correlate the activation state of erbB2 with the distribution pattern of the receptor, we activated SKBR3 cells with three different agents (4D5 antibody, EGF and heregulin). The 4D5 antibody is a partial agonist of erbB2 that induces tyrosine phosphorylation and down-regulation of erbB2 (Sarup et al., 1991). EGF and heregulin are known to directly or indirectly activate erbB2 and induce tyrosine phosphorylation of the protein (Holmes et al., 1992; Karunagaran et al., 1996; Nagy et al., 1998; Sliwkowski et al., 1994; Tzahar et al., 1997; Wallasch et al., 1995). We activated SKBR3 cells with EGF in the absence of serum for 30 minutes. Cells were only labeled afterwards to ensure that any fluorescence originated from the plasma membrane, and not from intracellular vesicles containing internalized erbB2 (Fig. 2D). EGF led to an increase in the size of erbB2 clusters according to each of the evaluation methods applied (Table 1, Figs 3, 4). Heregulin activation was carried out on SKBR3 cells in the absence of serum. The treatment also induced an increase in the size of erbB2 clusters (Figs 2F, 3, 4, 5; Table 1). However, heregulin-induced activation shifted the entire cluster population towards larger
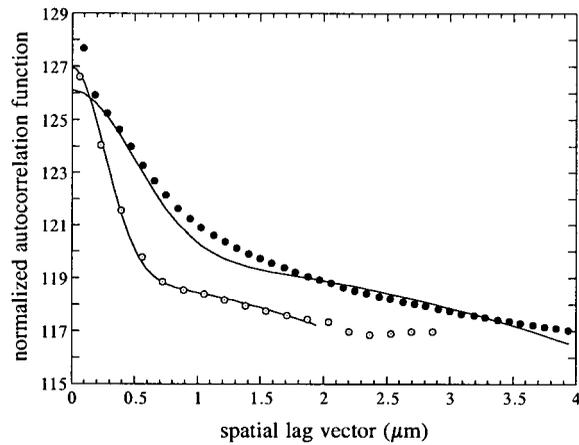
Fig. 5. Angle-averaged autocorrelation functions of quiescent and heregulin-activated SKBR3 cells. Quiescent (○) and heregulin-activated (●) SKBR3 cells were stained in situ with TAMRA-4D5 antibody. The angle-averaged autocorrelation function of the images was calculated. Data points were fitted to equation 1 (method 3). The fitted lines are also shown.

diameters, whereas in the case of the EGF ligand, some clusters were seemingly unaffected by exposure to the growth factor (Fig. 3). With the analysis according to method 3, the distinction between the two ligands was not so obvious. The automatic and manual segmentation procedures yield divergent results presumably due to differences in edge identification. However, the general tendency towards an increased erbB2 cluster diameter/area was universally present.

We also activated SKBR3 cells with the partially agonistic antibody, 4D5. In the first case, cells were activated with TAMRA-4D5 antibodies, and imaged in the SNOM without any further labeling, after fixation and dehydration. Although erbB2 is thought to be down-regulation deficient, it is slowly internalized (Baulida et al., 1996). In addition some controversy exists about the internalization of heregulin; some authors claim that it is not endocytosed (Baulida and Carpenter, 1997), while others find evidence for a quick translocation to the nucleus (Li et al., 1996). However, the assumption that the 4D5 antibody induces internalization of erbB2 is generally accepted (Sarup et al., 1991). Since SNOM can also register fluorescence from the far field albeit with diminished efficiency (Betzig and Chichester, 1993), the detected fluorescence may have had a partial contribution from internalized erbB2 proteins located in endocytotic vesicles underlying the plasma membrane. Therefore, in a second alternative procedure, cells were first activated with unlabeled 4D5 antibody and then stained with TAMRA-7C2 antibody, ensuring that any patchy appearance of fluorescence was not the result of erbB2 accumulation in intracellular vesicles (Fig. 2C). The results were the same using both staining protocols. In addition, we established that the staining patterns of nonactivated SKBR3 cells were similar upon labeling with TAMRA-4D5 or TAMRA-7C2 antibodies (data not shown), confirming that patterning was not specific for a particular antibody. As with EGF and heregulin, exposure of SKBR3 cells to the 4D5 antibody also caused an increase in the erbB2 cluster size distribution (Figs 2C, 3, 4, Table 1). The mean number of erbB2 proteins in a single cluster increased approximately

threefold with all of the activators on the surface of SKBR3 cells.

The influence of kinase inhibitor on the EGF-induced effect on erbB2 cluster size

In order to establish a direct link between increased tyrosine kinase activity and cluster size, we determined the size of erbB2 clusters in SKBR3 cells stimulated with EGF in the presence of PD153035, which specifically inhibits the tyrosine kinase activity of EGFR (Fry et al., 1994). Transmembrane signaling through the EGF receptor is markedly inhibited in the absence of tyrosine kinase activity of the protein (Fry et al., 1994). According to our results, the EGF-induced increase in the erbB2 cluster size was blocked by the inhibitor (Table 1, Fig. 2E). EGF primarily activates erbB1 tyrosine kinase activity, and erbB2 is only activated by secondary dimerization with the activated EGF receptor (Gamett et al., 1997). In the absence of EGF receptor tyrosine kinase activity the whole cascade phenomenon is inhibited (Gamett et al., 1997). The ability of the EGF receptor tyrosine kinase inhibitor to block erbB2 activation and increased cluster size further corroborates the link between receptor activation and increased large scale association.

Imaging of non-dehydrated SKBR3 cells with a confocal microscope

Although it has previously been shown that dehydration in itself does not influence the cluster size of membrane proteins (Hwang et al., 1998), we tested whether large-scale association of erbB2 is also present in cells kept under their near-physiological conditions. Quiescent SKBR3 cells were labeled with TAMRA-4D5 antibody, and imaged in the confocal laser scanning microscope without dehydration (Fig. 6). Inasmuch as results obtained with cells fixed with 1% formaldehyde were not significantly different from those of unfixed samples, we routinely used fixed cells during our experiments. Our results clearly indicate that erbB2 forms conspicuous clusters in non-dehydrated cells as well, the size of which coincided with that found in dehydrated cells. Since the lateral and axial resolution power of our confocal system was approximately 300 nm and 800 nm, respectively, a rigorous investigation of cluster size in quiescent and activated cells was not possible.

Concluding remarks

The ligand-induced formation of homo- and heterodimers among transmembrane proteins, and especially among members of the erbB family, is well established (Hynes and Stern, 1994; Weiss and Schlessinger, 1998). However, evidence has been reported for an intrinsic association of erbB1, the modulation of which by ligand is the process inducing activation of the receptor tyrosine kinase (Gadella and Jovin, 1995). In the present SNOM study, we demonstrate the large-scale clustering of the orphan erbB2 protein on the surface of quiescent and activated breast tumor cells, as well as on the surface of cells (CB2) ectopically expressing a transfected erbB2 protein. We confirmed the presence of erbB2 clusters in quiescent breast tumor cells with confocal microscopy of normally hydrated cells. The physical and chemical forces giving rise to such domains are under intensive investigation (Edidin, 1997; Friedrichson and Kurzchalia, 1998; Jacobson et al., 1995; Kusumi and Sako, 1996; Varma and Major, 1998).
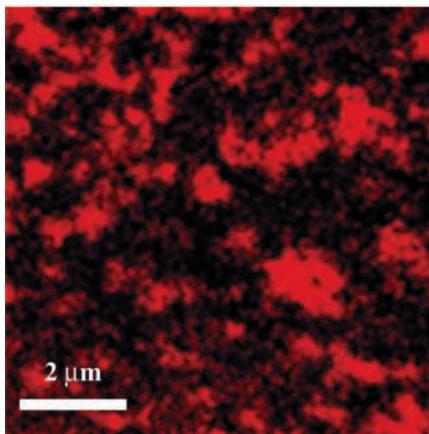
Fig. 6. Confocal image of quiescent, TAMRA-4D5-labeled SKBR3 cells. Cells were labeled without trypsinization on the surface of glass coverslips, and imaged with a confocal microscope without dehydration. The image shows an 8 µm wide, 800 nm thick section taken close to the surface of the coverslip.

One presumes that numerous intracellular and extracellular constraints and forces (e.g. interaction of cell surface proteins with the cytoskeleton or extracellular matrix) acting in and normal to the plane of the membrane influence the size and distribution of these clusters. In the case of the classical EGF receptor, one of these factors, interaction with the cytoskeleton, clearly has an important role in regulating the kinase activity of the protein (Gronowski and Bertics, 1993, 1995), pointing to the possible role of clustering in regulating cellular responses to growth factors.

The size of clusters seems to correlate with the activation state of erbB2. Large-scale clustering has also been described for other proteins in the plasma membrane (see Introduction). Since the activation of the erbB signaling network is accompanied by extensive interactions between receptors, their substrates and downstream effectors, it is probable that the concentration of erbB2 in clusters increases the efficiency of transmembrane signaling. A random distribution of a given number of erbB2 proteins in the membrane would decrease the local concentration of erbB2, and thereby increase the diffusion time required for generating direct receptor-receptor contact. Thus, clustering of signal transducing proteins may serve to decrease the lag time of activation. The size of erbB2 clusters increased with all the activation agents, and was even larger in quiescent CB2 cells, in which erbB2 exists in a pre-activated state. In addition, the EGF-induced increase in cluster size was dependent on the tyrosine kinase activity of the receptors, since it could be blocked with an EGF receptor-specific tyrosine kinase inhibitor. These findings argue for a general role of increased cluster size in erbB2-mediated signal transduction or, in the oncogenic state, aberrant and persistent mitogenic stimulation. The increased size probably reflects a recruitment of erbB2 and other proteins, potentiating synergistic effects. The process of receptor dimerization may be distinct from the formation of large-scale clusters in the sub-µm range containing hundreds of molecules. Both events may participate but have distinct roles in the activation of and downstream signaling by the receptors. According to one possible scenario, the first part in the two-step activation of the erbB signaling network is dimerization, which initiates receptor transphosphorylation. ErbB2 and other proteins are then recruited into the clusters, resulting in increased cluster size and high local concentration of signaling proteins. Although the exact composition of these protein clusters is unknown, we presume that they also contain other receptors, tyrosine kinase substrates and downstream effectors, and other 'structuring' elements like integrin or tetraspan molecules (Szöllősi et al., 1996). The precise mode of cell activation is determined by the composition of clusters, which is in turn influenced by the activating ligand. This point is under investigation with spectroscopic methods sensitive for co-expression and protein-protein interactions. Studies directed at the other erbB proteins in these clusters on the surface of quiescent and activated cells will shed light on another dimension of complexity in the network of interacting erbB proteins.

REFERENCES

Ahmad, I., Longenecker, M., Samuel, J. and Allen, T. M. (1993). Antibody-targeted delivery of doxorubicin entrapped in sterically stabilized liposomes can eradicate lung cancer in mice. *Cancer Res.* **53**, 1484-1488.

Alroy, I. and Yarden, Y. (1997). The ErbB signaling network in embryogenesis and oncogenesis: signal diversification through combinatorial ligand-receptor interactions. *FEBS Lett.* **410**, 83-86.

Bargmann, C. I., Hung, M.-C. and Weinberg, R. A. (1986). Multiple independent activations of the *neu* oncogene by a point mutation altering the transmembrane domain of p185. *Cell* **45**, 649-657.

Baselga, J., Tripathy, D., Mendelsohn, J., Baughman, S., Benz, C. C., Dantis, L., Sklarin, N. T., Seidman, A. D., Hudis, C. A. et al. (1996). Phase II study of weekly intravenous recombinant humanized anti-p185[HER2] monoclonal antibody in patients with HER2/*neu*-overexpressing metastatic breast cancer. *J. Clin. Oncol.* **14**, 737-744.

Baulida, J. and Carpenter, G. (1997). Heregulin degradation in the absence of rapid receptor-mediated internalization. *Exp. Cell Res.* **232**, 167-172.

Baulida, J., Kraus, M. H., Alimandi, M., Di Fiore, P. P. and Carpenter, G. (1996). All ErbB receptors other than the epidermal growth factor receptor are endocytosis impaired. *J. Biol. Chem.* **271**, 5251-5257.

Beerli, R. R., Graus Porta, D., Woods Cook, K., Chen, X., Yarden, Y. and Hynes, N. E. (1995). Neu differentiation factor activation of ErbB-3 and ErbB-4 is cell specific and displays a differential requirement for ErbB-2. *Mol. Cell. Biol.* **15**, 6496-6505.

Betzig, E. and Chichester, R. J. (1993). Single molecules observed by near-field scanning optical microscopy. *Science* **262**, 1422-1427.

Bielefeldt, H., Hörsch, G., Krausch, G., Lux-Steiner, M., Mlynek, J. and Marti, O. (1994). Reflection-scanning near-field optical microscopy and spectroscopy of opaque samples. *Appl. Phys. A: Solids Surf.* **59**, 103-108.

Courjon, D., Vigoureux, J. M., Spajer, M., Sarayeddine, K. and Leblanc, S. (1990). External and internal reflection near-field microscopy – experiments and results. *Appl. Opt.* **29**, 3734-3740.

Damjanovich, S., Vereb, G., Schaper, A., Jenei, A., Matkó, J., Starink, J. P., Fox, G. Q., Arndt-Jovin, D. J. and Jovin, T. M. (1995). Structural hierarchy in the clustering of HLA class I molecules in the plasma membrane of human lymphoblastoid cells. *Proc. Natl. Acad. Sci. USA* **92**, 1122-1126.

Edidin, M. (1997). Lipid microdomains in cell surface membranes. *Curr. Opin. Struct. Biol.* **7**, 528-532.

Fendly, B. M., Winget, M., Hudziak, R. M., Lipari, M. T., Napier, M. A. and Ullrich, A. (1990). Characterization of murine monoclonal antibodies

reactive to either the human epidermal growth factor receptor or HER2/neu gene product. *Cancer Res.* **50**, 1550-1558.

Friedrichson, T. and Kurzchalia, T. V. (1998). Microdomains of GPI-anchored proteins in living cells revealed by crosslinking. *Nature* **394**, 802-805.

Fry, D. W., Kraker, A. J., McMichael, A., Ambroso, L. A., Nelson, J. M., Leopold, W. R., Connors, R. W. and Bridges, A. J. (1994). A specific inhibitor of the epidermal growth factor receptor tyrosine kinase. *Science* **265**, 1093-1095.

Gadella, T. W., Jr. and Jovin, T. M. (1995). Oligomerization of epidermal growth factor receptors on A431 cells studied by time-resolved fluorescence imaging microscopy. A stereochemical model for tyrosine kinase receptor activation. *J. Cell Biol.* **129**, 1543-1558.

Gamett, D. C., Pearson, G., Cerione, R. A. and Friedberg, I. (1997). Secondary dimerization between members of the epidermal growth factor receptor family. *J. Biol. Chem.* **272**, 12052-12056.

Gronowski, A. M. and Bertics, P. J. (1993). Evidence for the potentiation of epidermal growth factor receptor tyrosine kinase activity by association with the detergent-insoluble cellular cytoskeleton: analysis of intact and carboxy-terminally truncated receptors. *Endocrinology* **133**, 2838-2846.

Gronowski, A. M. and Bertics, P. J. (1995). Modulation of epidermal growth factor receptor interaction with the detergent-insoluble cytoskeleton and its effects on receptor tyrosine kinase activity. *Endocrinology* **136**, 2198-2205.

Holmes, W. E., Sliwkowski, M. X., Akita, R. W., Henzel, W. J., Lee, J., Park, J. W., Yansura, D., Abadi, N., Raab, H., Lewis, G. D. et al. (1992). Identification of heregulin, a specific activator of p185erbB2. *Science* **256**, 1205-1210.

Hwang, J., Gheber, L. A., Margolis, L. and Edidin, M. (1998). Domains in cell plasma membranes investigated by near-field scanning optical microscopy. *Biophys. J.* **74**, 2184-2190.

Hwang, J., Tamm, L. K., Bohm, C., Ramalingam, T. S., Betzig, E. and Edidin, M. (1995). Nanoscale complexity of phospholipid monolayers investigated by near-field scanning optical microscopy. *Science* **270**, 610-614.

Hynes, N. E. and Stern, D. F. (1994). The biology of erbB-2/neu/HER-2 and its role in cancer. *Biochim. Biophys. Acta* **1198**, 165-184.

Jacobson, K., Sheets, E. D. and Simson, R. (1995). Revisiting the fluid mosaic model of membranes. *Science* **268**, 1441-1442.

Jenei, A., Varga, S., Bene, L., Mátyus, L., Bodnár, A., Bacsó, Z., Pieri, C., Gáspár, R., Jr., Farkas, T. and Damjanovich, S. (1997). HLA class I and II antigens are partially co-clustered in the plasma membrane of human lymphoblastoid cells. *Proc. Natl. Acad. Sci. USA* **94**, 7269-7274.

Karunagaran, D., Tzahar, E., Beerli, R. R., Chen, X., Graus Porta, D., Ratzkin, B. J., Seger, R., Hynes, N. E. and Yarden, Y. (1996). ErbB-2 is a common auxiliary subunit of NDF and EGF receptors: implications for breast cancer. *EMBO J.* **15**, 254-264.

Kenworthy, A. K. and Edidin, M. (1998). Distribution of glycosylphosphatidylinositol-anchored protein at the apical surface of MDCK cells examined at a resolution of <100 Å using imaging fluorescence resonance energy transfer. *J. Cell Biol.* **142**, 69-84.

Kirsch, A., Meyer, C. K. and Jovin, T. M. (1996). Integration of scanning probe microscopes with optical techniques. In *NATO Adv. Res. Workshop: Analytical use of fluorescent probes in oncology* (ed. E. Kohen and J. G. Hirschberg), pp. 317-323. New York: Plenum Press.

Kirsch, A. K., Meyer, C. K., Huesmann, H., Möbius, D. and Jovin, T. M. (1998a). Fluorescence SNOM of domain-structures of LB films containing electron-transfer systems. *Ultramicroscopy* **71**, 295-302.

Kirsch, A. K., Meyer, C. K. and Jovin, T. M. (1997). Shear force imaging of DNA in a near-field scanning optical microscope. *J. Microsc.* **185**, 396-401.

Kirsch, A. K., Schaper, A., Huesmann, H., Rampi, M. A., Möbius, D. and Jovin, T. M. (1998b). Scanning force and scanning near-field optical microscopy of organized monolayers incorporating a nonamphiphilic metal dyad. *Langmuir* **14**, 3895-3900.

Kirsch, A. K., Subramaniam, V., Striker, G., Schnetter, C., Arndt-Jovin, D. and Jovin, T. M. (1998c). Continuous wave two-photon scanning near-field optical microscopy. *Biophys. J.* **75**, 1513-1521.

Kusumi, A. and Sako, Y. (1996). Cell surface organization by the membrane skeleton. *Curr. Opin. Cell Biol.* **8**, 566-574.

Li, W., Park, J. W., Nuijens, A., Sliwkowski, M. X. and Keller, G. A. (1996). Heregulin is rapidly translocated to the nucleus and its transport is correlated with c-myc induction in breast cancer cells. *Oncogene* **12**, 2473-2477.

Matkó, J., Bushkin, Y., Wei, T. and Edidin, M. (1994). Clustering of class I HLA molecules on the surfaces of activated and transformed human cells. *J. Immunol.* **152**, 3353-3360.

Nagy, P., Bene, L., Balázs, M., Hyun, W. C., Lockett, S. J., Chiang, N. Y., Waldman, F. M., Feuerstein, B. G., Damjanovich, S. and Szöllősi, J. (1998). EGF-induced redistribution of erbB2 on breast tumor cells: Flow and image cytometric energy transfer measurements. *Cytometry* **32**, 120-131.

Press, M. F., Hung, G., Godolphin, W. and Slamon, D. J. (1994). Sensitivity of HER-2/neu antibodies in archival tissue samples: potential source of error in immunohistochemical studies of oncogene expression. *Cancer Res.* **54**, 2771-2777.

Sarup, J. C., Johnson, R. M., King, K. L., Fendly, B. M., Lipari, M. T., Napier, M. A., Ullrich, A. and Shepard, H. M. (1991). Characterization of an anti-p185HER2 monoclonal antibody that stimulates receptor function and inhibits tumor cell growth. *Growth Regul.* **1**, 72-82.

Sliwkowski, M. X., Schaefer, G., Akita, R. W., Lofgren, J. A., Fitzpatrick, V. D., Nuijens, A., Fendly, B. M., Cerione, R. A., Vandlen, R. L. and Carraway, K. L. (1994). Coexpression of erbB2 and erbB3 proteins reconstitutes a high affinity receptor for heregulin. *J. Biol. Chem.* **269**, 14661-14665.

Strawn, L. M. and Shawver, L. K. (1998). Tyrosine kinases in disease: overview of kinase inhibitors as therapeutic agents and current drugs in clinical trials. *Exp. Opin. Invest. Drugs* **7**, 553-573.

Szöllősi, J., Horejsi, V., Bene, L., Angelisova, P. and Damjanovich, S. (1996). Supramolecular complexes of MHC class I, MHC class II, CD20, and tetraspan molecules (CD53, CD81, and CD82) at the surface of a B cell line JY. *J. Immunol.* **157**, 2939-2946.

Tzahar, E., Pinkas Kramarski, R., Moyer, J. D., Klapper, L. N., Alroy, I., Levkowitz, G., Shelly, M., Henis, S., Eisenstein, M., Ratzkin, B. J. et al. (1997). Bivalence of EGF-like ligands drives the ErbB signaling network. *EMBO J.* **16**, 4938-4950.

Tzahar, E., Waterman, H., Chen, X., Levkowitz, G., Karunagaran, D., Lavi, S., Ratzkin, B. J. and Yarden, Y. (1996). A hierarchical network of interreceptor interactions determines signal transduction by Neu differentiation factor/neuregulin and epidermal growth factor. *Mol. Cell. Biol.* **16**, 5276-5287.

Varma, R. and Major, S. (1998). GPI-anchored proteins are organized in submicron domains at the cell surface. *Nature* **394**, 198-801.

Vereb, G., Meyer, C. K. and Jovin, T. M. (1997). Novel microscope-based approaches for the investigation of protein-protein interactions in signal transduction. *NATO ASI Series* **H102**, 49-52.

Wallasch, C., Weiss, F. U., Niederfellner, G., Jallal, B., Issing, W. and Ullrich, A. (1995). Heregulin-dependent regulation of HER2/neu oncogenic signaling by heterodimerization with HER3. *EMBO J.* **14**, 4267-4275.

Weiss, A. and Schlessinger, J. (1998). Switching signals on or off by receptor dimerization. *Cell* **94**, 277-280.